Published in final edited form as:
Anal Biochem. 2012 December 15; 431(2): 77–83. doi:10.1016/j.ab.2012.09.011.

Development of pyrethroid-like fluorescent substrates for glutathione *S*-transferase

Huazhang Huang[a,b], **Hongwei Yao**[a,b,c], **Jun-Yan Liu**[a,b], **Aman I. Samra**[a,b], **Shizuo G. Kamita**[a,b], **Anthony J. Cornel**[a], and **Bruce D. Hammock**[a,b,*]

[a]Department of Entomology, University of California, Davis, CA 95616, USA

[b]UC Davis Comprehensive Cancer Center, University of California, Davis, CA 95616, USA

Abstract

The availability of highly sensitive substrates is critical for the development of precise and rapid assays for detecting changes in glutathione *S*-transferase (GST) activity that are associated with GST-mediated metabolism of insecticides. In this study, six pyrethroid-like compounds were synthesized and characterized as substrates for insect and mammalian GSTs. All of the substrates were esters composed of the same alcohol moiety, 7-hydroxy-4-methylcoumarin, and acid moieties that structurally mimic some commonly used pyrethroid insecticides including cypermethrin and cyhalothrin. CpGSTD1, a recombinant Delta class GST from the mosquito *Culex pipiens,* metabolized our pyrethroid-like substrates with both chemical and geometric (i.e., the *cis*-isomers were metabolized at 2- to 5-fold higher rates than the corresponding *trans*-isomers) preference. A GST preparation from mouse liver also metabolized most of our pyrethroid-like substrates with both chemical and geometric preference but at 10- to 170-fold lower rates. CpGSTD1 and mouse GSTs metabolized CDNB, a general GST substrate, at more than 200-fold higher rates than our novel pyrethroid-like substrates. There was a 10-fold difference in the specificity constant (k_{cat}/K_M ratio) of CpGSTD1 for CDNB and those of CpGSTD1 for *cis*-DCVC and *cis*-TFMCVC suggesting that *cis*-DCVC and *cis*-TFMCVC may be useful for the detection of GST-based metabolism of pyrethroids in mosquitoes.

Keywords

glutathione *S*-transferase; GST; pyrethroid; fluorescent substrate

Introduction

Glutathione *S*-transferase (GST, EC 2.5.1.18) catalyzes nucleophilic attack of a wide range of compounds containing an electrophilic carbon, nitrogen, sulfur or oxygen atom by reduced glutathione (GSH) forming a glutathione conjugate (GS-conjugate) [1]. Although GSTs are primarily known for their ability to catalyze nucleophilic attack by GSH, GSTs can also catalyze the hydrolysis of esters, amides and sulfonamides [2–4] by attacking an electrophilic carbon, sulfur or phosphorus group. GSTs are also known to catalyze a

*Corresponding author: Bruce D. Hammock, Department of Entomology, University of California, 1 Shields Avenue, Davis, California 95616, Tel: 530-752-7519, Fax: 530-752-1537, bdhammock@ucdavis.edu.
[c]Current address: Institute of Insect Sciences, Zhejiang University, Hangzhou, 310029, China

dehalogenation reaction [3]. GSTs are involved in multiple biological functions including xenobiotic detoxification, clearance of oxidative stress products, protein transport, modulation of cell proliferation, and the induction of the apoptosis signaling pathway [1,5,6]. GSTs have been implicated to play important roles in insecticide resistance by metabolizing several classes of insecticides including organophosphates, carbamates, and organochlorines such as DDT [7–12]. GSTs also partially contribute to resistance to anti-cancer and anti-malarial drugs [13,14].

Numerous assays based on UV-spectrophotometric, fluorescent, luminescent, and colorimetric substrates are available for the detection of GST activity. The UV-spectrophotometric substrates 1-chloro-2,4-dinitrobenezene (CDNB) and 1,2-dichloro-4-nitrobenzene (DCNB) are commonly used, inexpensive substrates for the measurement of GST activity associated with a broad range of GST isozymes. In contrast to UV-spectrophotometric and colorimetric substrates, fluorescent and chemiluminescent substrates detect GST activity with enhanced sensitivity and reduced background. GST assays have been developed based on fluorescent substrates monochlorobimane [15], ammonium 4-chloro-7-sulfobenzofurazan [16], 7-chloro-4-nitrobenzo-2-oxa-1,3-diazole [17], 5-(pentafluorobenzoylamino) fluorescein [18], and 6-chloroacetyl-2-dimethylaminonaphthalene [19]. A fluorescent assay specifically for the detection of microsomal GST activity based on the fluorescent reporter rhodamine has also been developed [20]. Chemiluminescent substrates based on sulfonate esters are also available for use in high throughput GST assays [21,22]. In this study, six esters (Fig. 1) were designed for the detection of GST activity. Our ester compounds are all composed of the same alcohol moiety, 7-hydroxy-4-methylcoumarin. The acid moieties of our ester compounds mimic some commonly used pyrethroid insecticides including permethrin and bifenthrin (type I pyrethroids) and cypermethrin and cyhalothrin (type II pyrethroids). Because our compounds are esters, they have potential dual function for the detection of GST and esterase activities.

Pyrethroid insecticides are widely used to control pest insects of agriculture and insects that vector human and veterinary diseases [23]. Unfortunately, resistance to pyrethroid insecticides is found in numerous insects including disease vector mosquitoes and agriculturally important caterpillars. Target site insensitivity and the elevation of detoxification enzymes (i.e., carboxylesterases and oxidases) are currently considered the primary mechanisms of pyrethroid resistance [9,23,24]. The functional role of GSTs in pyrethroid resistance, however, has not been well studied in part because of the lack of acceptably selective and inexpensive high-throughput activity assays that target GST activity associated with pyrethroid metabolism. The pyrethroid-like fluorescent substrates developed in this study will potentially lead to a new generation of rapid and highly sensitive assays for the detection of elevated GST activity associated with resistance to pyrethroid insecticides.

Materials and methods

General procedure for preparation of pyrethroid-like esters

Each pyrethroid-like ester was generated by slowly adding the appropriate acid chloride (10.5 mmol) and 4-methylmorpholine (10.5 mmol) to an ice-cooled solution of 7-hydroxy-4-methylcoumarin (10 mmol) in anhydrous CH_2Cl_2 (20 ml). The reaction was allowed to slowly warm to room temperature and continuously stirred overnight. The reaction mixture was then washed with a saturated NaCl solution and extracted three times (20 ml per extraction) with ethyl acetate. The combined organic phase was dried with $MgSO_4$. A crude solid product was obtained after filtration and evaporation under reduced pressure. The crude product was purified by column chromatography using silica gel (32–63 μm,

Dynamic Adsorbents, Norcross, GA, USA) using a mobile phase of hexanes:ethyl acetate (9:1). The yield of each pyrethroid-like ester was between 85% and 92%.

Structural characterization of the synthesized compounds

Structural identification was based on both ^{1}H-NMR and GC/MS analyses. Proton NMR spectra were acquired from a Mercury 300 spectrometer (Varian, Palo Alto, CA, USA). Chemical shift values are represented in ppm downfield from an internal standard (trimethylsilane). Signal multiplicities are represented as singlet (s), doublet (d), double doublet (dd), triplet (t), quartet (q), quintet (quint), multiplet (m), broad (br), and broad singlet (brs). Melting points were determined on a Uni-Melt apparatus (Thomas Scientific, Swedesborogh, NJ) and are uncorrected. Chemical purity of the final products was supported by the spectral analysis described above. A sharp melting point and a single spot by TLC (250 micron silica gel F254 plates using a solvent system of hexanes:ethyl acetate (4:1)) when detected at a wavelength of 254 nm, and lack of a 7-hydroxy-4-methylcoumarin signal when detected at a wavelength of 360 nm were taken as additional indications of purity. The characteristics of our six compounds are given below.

4-Methyl-2-oxo-2H-chromen-6-yl, 2, 2, 3, 3-tetramethylcyclopropanecarboxylate (**TMC**): white powder, mp 119.1–122.0°C, ^{1}H NMR ($CDCl_3$): δ 7.57 (d, *J*=8.4 Hz, 1H), 7.05–7.10 (m, 2H), 6.25 (s, 3H, CH_3), 2.42 (s, 3H, CH_3), 1.44 (s, 1H), 1.29 (s, 6H, $2CH_3$), 1.28 (s, 6H, $2CH_3$).

4-Methyl-2-oxo-2H-chromen-6-yl, *cis*/*trans*- 2,2-dimethyl-3-(2-methylprop-1-enyl) cyclopropanecarboxylate (**DMVC**): white powder, mp 99.6–107.6°C, ^{1}H NMR ($CDCl_3$): δ 7.57 (d, *J*=8.4 Hz, 1H, *trans*), 7.56 (d, *J*=8.4 Hz, 1H, *cis*), 7.04–7.11 (m, 2H), 6.25 (s, 3H, CH_3), 5.32 (d, *J*=8.4 Hz, 1H, *cis*), 4.94 (d, *J*=8.4 Hz, 1H, *trans*), 2.42 (s, 3H, CH_3), 2.20 (dd, J_1=8.4 Hz, J_2=5.1 Hz, 1H, *trans*), 2.09 (t, *J*=8.4 Hz, 1H, *cis*), 1.90 (d, *J*=8.4 Hz, 1H, *trans*), 1.75 (s, 3H, CH_3), 1.73 (s, 3H, CH_3), 1.64 (d, *J*=5.1 Hz, 1H, *trans*), 1.35 (s, 3H, CH_3), 1.23 (s, 3H, CH_3).

4-Methyl-2-oxo-2H-chromen-6-yl, *cis*-3-(2,2-dichlorovinyl)-2,2-dimethylcyclo propanecarboxylate (***cis*-DCVC**): white crystal, mp 149.1–151.0°C, ^{1} 7.60 (d, H NMR ($CDCl_3$): δ *J*=8.4 Hz, 1H), 7.06–7.12 (m, 2H), 6.26 (s, 3H, CH_3), 6.20 (d, *J*=8.4 Hz, 1H), 2.42 (s, 3H, CH_3), 2.20 (dd, J_1=8.4 Hz, J_2=5.1 Hz, 1H), 2.09 (d, *J*=5.1 Hz, 1H), 1.35 (s, 3H, CH_3), 1.29 (s, 3H, CH_3).

4-Methyl-2-oxo-2H-chromen-6-yl, *trans*-3-(2,2-dichlorovinyl)-2,2-dimethyl cyclopropanecarboxylate (***trans*-DCVC**): spongy white powder, mp 133.4–135.1°C, ^{1}H NMR ($CDCl_3$): δ 7.59 (d, *J*=8.4 Hz, 1H), 7.06–7.12 (m, 2H), 6.26 (s, 3H, CH_3), 5.68 (d, *J*=8.4 Hz, 1H), 2.42 (s, 3H, CH_3), 2.20 (dd, J_1=8.4 Hz, J_2=5.1 Hz, 1H), 1.85 (d, *J*=5.1 Hz, 1H), 1.38 (s, 3H, CH_3), 1.29 (s, 3H, CH_3).

4-Methyl-2-oxo-2H-chromen-6-yl, *cis*-3-((Z)-2-chloro-3,3,3-trifluoroprop-1-enyl)-2,2-dimethylcyclopropanecarboxylate (***cis*-TFMCVC**): fine white powder, mp 139.5–140.6°C, ^{1}H NMR ($CDCl_3$): δ 7.61 (d, *J*=9.0 Hz, 1H), 7.07–7.13 (m, 2H), 6.86 (d, *J*=9.0 Hz, 1H), 6.26 (s, 3H, CH_3), 2.42 (s, 3H, CH_3), 2.36 (t, *J*=9.0 Hz, 1H), 2.24 (d, *J*=9.0 Hz, 1H), 1.41 (s, 3H, CH_3), 1.35 (s, 3H, CH_3).

4-Methyl-2-oxo-2H-chromen-6-yl, 1*R trans*-3-((Z)-2-chloro-3,3,3-trifluoroprop-1-enyl)-2,2-dimethylcyclopropanecarboxylate (**1*R trans*-TFMCVC**): white powder, mp 133.6–135.0°C, ^{1}H NMR ($CDCl_3$): δ 7.60 (d, *J*=8.4 Hz, 1H), 7.07–7.13(m, 2H), 6.27 (s, 3H, CH_3), 6.21 (d, *J*=9.0 Hz, 1H), 2.53 (dd, J_1=9.0 Hz, J_2=5.1 Hz, 1H), 2.44 (s, 3H, CH_3), 2.03(d, *J*=5.1 Hz, 1H), 1.43 (s, 3H, CH_3), 1.34 (s, 3H, CH_3).

Preparation of recombinant mosquito and mouse GSTs and confirmation of GST activity

CpGSTD1, a recombinant Delta class GST [25] from the pyrethroid-resistant mosquito *Culex pipiens pipiens* L from Marin, California [26], was expressed in BL21Pro cells (Clontech Laboratories, Mountain View, CA, USA) and purified using GSH agarose (Sigma-Aldrich, St. Louis, MO, USA) as described previously [25,27]. Murine cytosolic GSTs were isolated from the livers of four 8-week-old C57BL/6 mice (Charles River Laboratories International, Wilmington, MA, USA) each with a mass of 22 to 25 g. The liver of each mouse was removed immediately after sacrifice and frozen. For GST extraction, the frozen livers were allowed to quickly thaw in a room temperature water bath, and then homogenized on ice in 100 mM sodium phosphate, pH 7.4, buffer by multiple 20 s-long pulses of a Polytron (Brinkmann Instruments, Westbury, NY, USA) homogenizer set at a speed of 7. The homogenate was centrifuged at 12,000 × *g* for 20 min, and the supernatant was subjected to affinity purification using GSH agarose as previously [27]. The purity of the recombinant mosquito and mouse GSTs was determined by SDS-PAGE separation using 10% NuPAGE Bis-Tris gels (Invitrogen, Carlsbad, CA, USA) and NuPAGE MOPS SDS running buffer (Invitrogen) followed by staining with Simply Blue SafeStain (Invitrogen) following the manufacturer's protocol. The GST activity of the mosquito and murine protein preparations were confirmed with the general GST substrates CDNB and DCNB as described previously [25]. The presence of esterase activity in the protein preparations was investigated using *ρ*-nitrophenyl acetate (*ρ*-NPA) as described previously [28,29] and by the use of an esterase inhibitor as described below.

Standard fluorescent GST assay

The ability of the recombinant mosquito and mouse GSTs to metabolize the pyrethroid-like esters (Fig. 1) was determined in a 200 μl assay in the wells of a black, flat bottom, 96-well plate (Greiner Bio-One, Monroe, NC, USA) at 34°C. Formation of 7-hydroxy-4-methyl coumarin, a metabolite of our pyrethroid-like ester compounds, was measured by spectrophotometry with an excitation wavelength of 330 nm and an emission wavelength of 460 nm with monitoring at 27 s intervals for 10 min using a Spectra Max M2 spectrophotometer (Molecular Devices, Sunnyvale, CA, USA). Each reaction contained GST (720 ng of CpGSTD1 or 1,400 ng of murine GSTs), 50 μM fluorescent substrate, 750 μM GSH, and 0.5% (v/v) di(ethylgylcerol)ethyl ether (DEGEE) in 90 mM sodium phosphate, pH 7.4, buffer. The reaction mixture was pre-incubated at 34°C for 10 min with shaking (for 3 s) at 27 s intervals prior to the addition of the substrate. Each assay was performed in quadruplicate wells of the same 96-well plate. Quadruplicate wells containing buffer only, buffer plus GSH (750 μM) or buffer plus GST protein (720 ng or 1,400 ng as appropriate) were included on each plate as controls. GST-dependent activity was calculated by subtracting the background activity in control wells containing only GSH from the activity in wells containing GST enzyme and GSH. The potential presence of esterases in the GST preparations was tested by the addition of the esterase inhibitor 3-octylthio-1,1,1-trifluoropropan-2-one (OTFP) [30] to the standard GST assay (these assays also contained 0.5% DMSO). The OTFP (1 μM final concentration) was incubated with the enzyme for 10 min at 34°C prior to the addition of substrate.

Determination of kinetic constants of the fluorescent substrates with CpGSTD1

V_{max} and Michaelis constant (K_m) values were determined with CpGSTD1 and six concentrations each of *cis*-DCVC, *trans*-DCVC, *cis*-TFMCVC or 1*R trans*-TFMCVC by linear regression analysis using the SigmaPlot Enzyme Kinetics Module 1.1 (Systat Software, San Jose, CA, USA). The k_{cat} values of CpGSTD1 were determined using an estimated molecular weight of 23,777 Daltons. For these experiments, the standard fluorescent GST described above was modified so that each 200 μl reaction contained 184 ng of CpGSTD1, various concentrations of the above mentioned four substrates (1, 2, 3.9,

7.8, 15.6 or 31.2 μM), 750 μM GSH, and 2% (v/v) DEGEE in 90 mM sodium phosphate, pH 7.4, buffer. For each substrate and substrate concentration, control wells containing everything but CpGSTD1 were used to determine background hydrolysis levels.

Effect of GSH and protein concentrations on the metabolism of cis-DCVC by CpGSTD1

For the experiments to determine the effect of GSH concentration on the metabolism of *cis*-DCVC, the standard fluorescent GST assay described above was modified so that each 200 μl reaction contained 79 ng of CpGSTD1, 50 μM *cis*-DCVC, various concentrations of GSH (0.78, 3.12, 6.25, 12.5, 25, 50, 100, 200, 750 or 1,500 μM), and 2% (v/v) DEGEE in 90 mM sodium phosphate, pH 7.4, buffer. For the experiments to determine the effects of protein concentration on the metabolism of *cis*-DCVC by CpGSTD1, the standard fluorescent GST assay described above was modified so that each 200 μl reaction contained various amounts of CpGSTD1 (23.5, 47, 94, 141 or 188 ng), 50 μM *cis*-DCVC, 750 μM GSH, and 2% (v/v) DEGEE in 90 mM sodium phosphate, pH 7.4, buffer.

Inhibition of CpGSTD1 by Bivalent GST inhibitor

The median inhibitory concentration (IC_{50}) of the GST inhibitor Bivalent GST inhibitor (EA-Asp-Gly-AMAB-Gly-Asp-EA; where EA = ethacrynic acid and AMAB = 3,5-aminomethylbenzoic acid amide) [31] was determined using the standard fluorescent GST assay described above so that each 200 μl reaction contained 720 ng of CpGSTD1, various concentration of the inhibitor (0, 3, 6.1, 12.2, 24.4, 48.8, 98.5 or 195 nM), 50 μM *cis*-DCVC, 750 μM GSH, and 2% (v/v) DEGEE in 90 mM sodium phosphate, pH 7.4, buffer. The IC_{50} values were determined by a linear regression analysis as described above.

LC/MS analysis of the metabolites produced by CpGSTD1 metabolism of the fluorescent substrates

The predicted final products of the metabolism of the pyrethroid-like substrates by GST are 7-hydroxy-4-methylcoumarin and a corresponding GSH-conjugated pyrethroid-like acid. LC/MS coupled with electrospray ionization (LC/MS ESI^+) was used to support the expected 1:1 correlation between the 7-hydroxy-4-methylcoumarin and GS-conjugate acid metabolites as well as to determine the mass of the GS-conjugates. For these experiments, the standard fluorescent GST assay was quenched at the completion of the 10 min-long reaction by the addition of acetonitrile. After addition of the acetonitrile, the reaction mixture was shaken for 10 s and the resulting mixture was immediately frozen at −78°C prior to LC/MS ESI^+ analysis. Chromatographic separation was performed at 25°C on a Waters (Waters Corporation, Milford, MA, USA) high-performance liquid chromatograph equipped with a Waters Atlantis dC18 3 μm (2.1 mm × 150 mm) column. The solvent system consisted of water/acetonitrile/formic acid (899/100/1 (v/v), solvent A) and acetonitrile/formic acid (999/1 (v/v); solvent B). The mobile phase (flow rate of 0.4 ml min^{-1}) began at 0% solvent B for 5 min, and then was linearly increased to 100% solvent B over 27 min and then run in solvent B for 7 min, and finally returned to 0% solvent B over 1 min. The injection volume was 10 μl and the samples were kept at 4°C in an auto sampler. GS-conjugates were detected by positive mode electrospray ionization time of flight (TOF) mass spectrometry in full scan mode (*m/z* 100–1500 Da) using a Micromass LCT Mass Spectrometer (Waters Corporation). The flow rate of the nitrogen gas was fixed at 30 l h^{-1} for the cone gas flow and 950 l h^{-1} for the desolvation gas flow. Electrospray ionization was performed with a capillary voltage set at 2700 V and an extractor fixed at 2.0 V. The source and desolvation temperatures were set at 110°C and 300°C, respectively.

Results

Specific activity of CpGSTD1 and mouse GSTs toward the pyrethroid-like fluorescent substrates

The purity of TMC, *cis*-DCVC, *trans*-DCVC, *cis*-TFMCVC, and 1R *trans*-TFMCVC was estimated to be greater than 98% on the basis of ^{1}H-NMR, TLC, and GC/MS analyses. On the basis of these analyses, DMVC appeared to be a mixture of *cis* and *trans* isomers (45% *cis*-DMVC and 55% *trans*-DMVC). CpGSTD1 selectively metabolized all six of these pyrethroid-like esters with specific activities that ranged from approximately 10 to 230 nmol min^{-1} mg^{-1} (Table 1). CpGSTD1 metabolized the *cis*-isomers of DCVC and TFMCVC at approximately 2- to 5-fold faster rates than their corresponding *trans*-isomers. CpGSTD1 showed up to 20-fold lower specific activity for TMC and DMVC in comparison to DCVC and TMCVC. The mouse GST preparation also appear to show significantly lower specific activity (1 to 4 nmol min^{-1} mg^{-1}) with both the *cis*- and *trans*-isomers of DCVC and TFMCVC, and no detectable metabolism of TMC and DMVC (Table 1). The mouse GST preparation also showed no apparent geometric preference for DCVC, but metabolized the *trans*-isomer of TFMCVC at 2.9-fold faster rates than the corresponding *cis*-isomer. Since the mouse GST preparation likely contained multiple GST isoforms, it's possible that one or more of these isoforms possesses significantly higher specific activity for these substrates.

Several lines of evidence showed that the metabolism of our pyrethroid-like substrates was CpGSTD1-specific and not due to esterase contamination in the protein preparation. Firstly, the CpGSTD1 preparation showed no detectable activity toward the general esterase substrates ρ-NPA under the same reaction conditions that were tested with the pyrethroid-like ester compounds. Secondly, the CpGSTD1 preparation was not inhibited by OTFP, a potent inhibitor of general esterases, at concentrations of up to 1 μM. It was, however, inhibited by a selective bivalent GST inhibitor with an IC_{50} of 34.4 ± 4.8 nM. Thirdly, the ability of CpGSTD1 to metabolize *cis*-DCVC was dependent upon GSH concentration (Figs. 2), and there was an excellent (r^2 = 0.981) correlation between the protein concentration of the CpGSTD1 preparation (within a range of 0 to 188 ng per 200 μl) and activity (Fig. 3). Additionally, when 1.2 μg of the CpGSTD1 preparation was separated by SDS-PAGE only a single ca. 24 kDa band was visible following staining (Fig. S1).

Enzyme kinetic analysis of CpGSTD1 with the pyrethroid-like fluorescent substrates

CpGSTD1 metabolized the *cis*- and *trans*-isomers of DCVC and TFMCVC with maximum velocity (V_{max}) values in the range of 50 to 490 nmol min^{-1} mg^{-1} (Table 2). The V_{max} of CpGSTD1 for the *cis*-isomers of both DCVC and TFMCVC were 3- and 9-fold higher, respectively, than the corresponding *trans*-isomer. In contrast to the pyrethroid-like fluorescent substrates, CpGSTD1 metabolized CDNB and DCNB with significantly higher (209- and 5-fold, respectively) higher V_{max} values of 102,000 and 2,320 nmol min^{-1} mg^{-1}, respectively (Table 2). These higher rates, however, required relatively high substrate concentrations as indicated by significantly higher (up to 140-fold) K_M values (Table 2). The turnover (k_{cat}) of all of the pyrethroid-like substrates was very slow (Table 2). In a manner consistent with the specific activity data of CpGSTD1 (Table 1), the specific activity constants (k_{cat}/K_M ratio) of CpGSTD1 for *cis*-DCVC and *cis*-TFMCVC were 2- and 5-fold higher, respectively, in comparison to the corresponding trans isomer.

Analysis of the metabolites of the pyrethroid-like fluorescent substrates

Following the incubation of CpGSTD1 with each of our pyrethroid-like substrates under our "standard fluorescent GST assay" conditions, LC/MS ESI$^+$ analysis indicated that the mass (*m/z*) of the GS-conjugates of DMVC, *cis*-/*trans*-DCVC and *cis*-/1*R trans*-TFMCVC were 458, 498, and 532, respectively (Fig. 4). A direct correlation was found between the results

of the LC/MS ESI$^+$ analysis and the metabolic activity of CpGSTD1 for our pyrethroid-like fluorescent substrates. In a manner consistent with the specific activity results, there was no detectable metabolism of TMC on the basis of a mass spectra scan for a molecular mass (*m/z*) of 432, which is the putative mass of the GS-conjugation of TMC.

Discussion

In this study, six ester-containing pyrethroid-like fluorescent substrates were developed for the detection of GST activity. The acid moiety of four of our substrates (*cis*-/*trans*-DCVC and *cis*-/1*R trans*-TFMCVC) were designed to mimic the commonly used type I pyrethroid insecticides permethrin and bifenthrin, respectively, and the type II pyrethroids cypermethrin and cyhalothrin, respectively. The insect GST appeared to metabolize these substrates at significantly higher rates than the mouse GST preparation. However, the mouse GST preparation was made from whole livers and likely contained multiple GST isoforms. Thus, it is possible that one of these isoforms, if purified, could metabolize our substrates with specific activity that is equal to or higher than that of CpGSTD1. On the basis of specific activity values, CpGSTD1 showed the following preference for our pyrethroid-like substrates: *cis*-TFMCVC > *cis*-DCVC > *trans*-DCVC > 1*R trans*-TFMCVC > DMVC > TMC. The mouse GSTs on the other hand showed no detectable metabolism of DMVC and TMC (a mimic of uncommon pyrethroid), and very little chemical or geometric preference for the other pyrethroid-like substrates.

There are at least three possible metabolic fates of our pyrethroid-like esters following metabolism by GST (Fig. 5). Mechanistically these potential metabolic pathways take advantage of the fact that the alcohol moiety (i.e., 7-hydroxy-4-methylcoumarin) that is found in all of our fluorescent substrates is a very good leaving group. In our first proposed pathway, GST catalyzes the dehalogenation of our pyrethroid-like substrates in a manner similar to that of hexachlorobutadiene [32]. If this occurs, an intermediate conjugate with a mass of 638 should have been detected by LC/MS ESI$^+$. The mass profiles of the GS-conjugates from our pyrethroid-like esters, however, suggested that this type of mechanism does not occur. In our second proposed pathway, GST adds GSH by a Michael addition reaction to the electrophilic (halogen-attached) carbon of the vinyl group of our pyrethroid-like substrates; this will cause the second carbon of the vinyl group to become nucleophilic. This second carbon will then be potentially close enough to the carbonyl of the ester to initiate a nucleophilic attack so that a GS-conjugate is formed and 7-hydroxy-4-methylcoumarin is released. Finally, in our third proposed pathway, GST catalyzes the thiolysis of our pyrethroid-like substrates as they do with the *p*NPA [2–4], this reaction will also form a GS-conjugate and release 7-hydroxy-4-methylcoumarin. The mass of the GS-conjugate from the both 2nd and 3rd potential mechanisms should be identical, and both proposed mechanisms will result in the release of 7-hydroxy-4-methylcoumarin. In order to exclude one of these to potential mechanisms, we attempted to purify the potential GS-conjugate for further structural characterization. Both of the GS-conjugate structures, however, appeared to be unstable and our purification efforts were unsuccessful.

Synthetic pyrethroids are highly insect selective insecticides that do not accumulate in the environment and have a half century-long track record of safe and effective use. The occurrence of pyrethroid resistance, however, is an ongoing problem that requires appropriate management and tools for detection so that the effective use of these compounds can be continued. Numerous studies show that GST activity and/or *gst* gene expression levels are quantitatively increased in pyrethroid resistant insects [25,33–38]. These studies generally suggest that the role of GST in insecticide resistance is as an antioxidant defense agent or binding protein [33,36,37]. In contrast, monooxygenases and esterases have been shown to play direct roles in pyrethroid resistance by metabolizing pyrethroids [39–43].

There is, however, one example of the direct metabolism of the pyrethroid tetramethrin by a non-insect GST [44].

The ability to quickly, accurately, and quantitatively detect target site mutations and elevated levels of pyrethroid detoxification enzymes is a critical component of the continued effective use of pyrethroids. We hope to develop our pyrethroid-like substrates, in particular *cis*-TFMCVC and *cis*-DCVC, for use in simple fluorescent assays to detect elevated levels of GST and/or esterase activity that may be associated with resistance to permethrin/cypermethrin and bifenthrin/cyhalothrin, and other commonly used synthetic pyrethroids.

Supplementary Material

Refer to Web version on PubMed Central for supplementary material.

Acknowledgments

The authors thank Drs. Jun Yang and Christophe Morisseau for assistance during this study, Professor Marilyn M. Olmstead and Ms. Christine M. Beavers in Chemistry Department of University of California, Davis, for running X-ray crystallography. We also thank Drs. William M. Atkins and Sumit S. Mahajan in the Chemistry Department of University of Washington for generously providing the bivalent GST inhibitor. All experiments involving mice were performed according to a protocol approved by the UC Davis Animal Use and Care Committee. This work was funded by National Institute of Environmental Health Sciences (NIEHS) grant #R01 ES002710, NIEHS Superfund Basic Research Program grant #P42 ES04699, and Mosquito Research Foundation grants #07-020-2-1 and #201222676.

Abbreviations used

GST	glutathione *S*-transferase
GS-conjugate	glutathione conjugate
CpGSTD1	recombinant Delta class GST from *Culex pipiens pipiens*
TMC	4-methyl-2-oxo-2H-chromen-6-yl, 2, 2, 3, 3-tetramethylcyclopropanecarboxylate
DMVC	4-methyl-2-oxo-2H-chromen-6-yl, *cis*/*trans*- 2,2-dimethyl-3-(2-methylprop-1-enyl) cyclopropanecarboxylate
***cis*-DCVC**	4-methyl-2-oxo-2H-chromen-6-yl, *cis*-3-(2,2-dichlorovinyl)-2,2-dimethylcyclo propanecarboxylate
***trans*-DCVC**	4-methyl-2-oxo-2H-chromen-6-yl, *trans*-3-(2,2-dichlorovinyl)-2,2-dimethyl cyclopropanecarboxylate
***cis*-TFMCVC**	4-methyl-2-oxo-2H-chromen-6-yl, *cis*-3-((Z)-2-chloro-3,3,3-trifluoroprop-1-enyl)-2,2-dimethylcyclopropanecarboxylate
1*R trans*-TFMCVC	4-methyl-2-oxo-2H-chromen-6-yl, 1*R trans*-3-((Z)-2-chloro-3,3,3-trifluoroprop-1-enyl)-2,2-dimethylcyclopropanecarboxylate
CDNB	1-chloro-2,4-dinitrobenzene
DCNB	1,2-dichloro-4-nitrobenzene
ρ-NPA	ρ-nitrophenyl acetate
OTFP	3-octylthio-1,1,1-trifluoropropan-2-one
DEGEE	di(ethylgylcerol)ethyl ether
DMSO	dimethyl sulfoxide

IC_{50}	median inhibitor concentration

References

1. Hayes JD, Flanagan JU, Jowsey IR. Glutathione transferases. Ann Rev Pharmacol Toxicol. 2005; 45:51–88. [PubMed: 15822171]
2. Satoh K. The high nonenzymatic conjugation rates of some glutathione *S*-transferase (GST) substrates at high glutathione concentrations. Carcinogenesis. 1995; 16:869–874. [PubMed: 7728969]
3. Mitchell AE, Zheng J, Hammock BD, Lo Bello M, Jones AD. Structural and functional consequences of haloenol lactone inactivation of murine and human glutathione *S*-transferase. Biochem. 1998; 37:6752–6759. [PubMed: 9578559]
4. Ibarra C, Grillo MP, Lo Bello M, Nucettelli M, Bammler TK, Atkins WM. Exploration of in vitro pro-drug activation and futile cycling by glutathione *S*-transferases: thiol ester hydrolysis and inhibitor maturation. Arch Biochem Biophys. 2003; 414:303–311. [PubMed: 12781783]
5. McIlwain CC, Townsend DM, Tew KD. Glutathione *S*-transferase polymorphisms: cancer incidence and therapy. Oncogene. 2006; 25:1639–1648. [PubMed: 16550164]
6. Tew KD. Redox in redux: emergent roles for glutathione *S*-transferase P (GSTP) in regulation of cell signaling and *S*-glutathionylation. Biochem Pharmacol. 2007; 73:1257–1269. [PubMed: 17098212]
7. Clark AG, Smith JN, Speir TW. Cross specificity in some vertebrate and insect glutathione transferases with methyl parathion (dimethyl *p*-nitrophenyl phosphorothionate), 1-chloro-2,4-dinitro-benzene and S-crotonyl-N-acetylcysteamine as substrates. Biochem J. 1973; 135:385–392. [PubMed: 4772267]
8. Motoyama N, Dauterman WC. Interstrain comparison of glutathione-dependent reactions in susceptible and resistant houseflies. Pest Biochem Physiol. 1975; 5:489–495.
9. Hemingway J, Ranson H. Insecticide resistance in insect vectors of human disease. Ann Rev Entomol. 2000; 45:371–391. [PubMed: 10761582]
10. Ranson H, Rossiter L, Ortelli F, Jensen B, Wang XL, Roth CW, Collins FH, Hemingway J. Identification of a novel class of insect glutathione *S*-transferases involved in resistance to DDT in the malaria vector *Anopheles gambiae*. Biochem J. 2001; 359:295–304. [PubMed: 11583575]
11. Wei SH, Clark AG, Syvanen M. Identification and cloning of a key insecticide-metabolizing glutathione *S*-transferase (MdGST-6A) from a hyper insecticide-resistant strain of the housefly *Musca domestica*. Insect Biochem Mol Biol. 2001; 31:1145–1153. [PubMed: 11583927]
12. Sun, C-N.; Huang, S-Y.; Hu, N-T.; Chung, W-Y. Biochemical Sites of Insecticide Action and Resistance. Sun, C-N.; Huang, S-Y.; Hu, N-T.; Chung, W-Y., editors. Springer-Verlag; Berlin: 2001. p. 239-254.
13. Mahajan S, Atkins WM. The chemistry and biology of inhibitors and pro-drugs targeted to glutathione *S*-transferases. Cell Mol Life Sci. 2005; 62:1221–1233. [PubMed: 15798895]
14. Zhao GS, Wang XB. Advances in antitumor agents targeting glutathione *S*-transferase. Curr Med Chem. 2006; 13:1461–1471. [PubMed: 16719788]
15. Rice GC, Bump EA, Shrieve DC, Lee W, Kovacs M. Quantitative analysis of cellular glutathione by flow cytometry utilizing monochlorobimane: some applications to radiation and drug resistance in vitro and in vivo. Cancer Res. 1986; 46:6105–6110. [PubMed: 3779630]
16. Bolton RM, Haritos VS, Whitehouse MW, Ahokas JT. Ammonium 4-chloro-7-sulfobenzofurazan: a fluorescent substrate highly specific for rat glutathione *S*-transferase subunit 3. Anal Biochem. 1994; 216:418–423. [PubMed: 8179198]
17. Ricci G, Caccuri AM, Lobello M, Pastore A, Piemonte F, Federici G. Colorimetric and fluorometric assays of glutathione transferase based on 7-chloro-4-nitrobenzo-2-Oxa-1,3-diazole. Anal Biochem. 1994; 218:463–465. [PubMed: 8074309]
18. Arttamangkul S, Bhalgat MK, Haugland RP, Diwu ZJ, Liu JX, Klaubert DH, Haugland RP. 5-(Pentafluorobenzoylamino)fluorescein: a selective substrate for the determination of glutathione

concentration and glutathione *S*-transferase activity. Anal Biochem. 1999; 269:410–417. [PubMed: 10222018]

19. Svensson R, Greno C, Johansson AS, Mannervik B, Morgenstern R. Synthesis and characterization of 6-chloroacetyl-2-dimethylaminonaphthalene as a fluorogenic substrate and a mechanistic probe for glutathione transferases. Anal Biochem. 2002; 311:171–178. [PubMed: 12470677]
20. Alander J, Johansson K, Heuser VD, Farebo H, Jarvliden J, Abe H, Shibata A, Ito M, Ito Y, Morgenstern R. Characterization of a new fluorogenic substrate for microsomal glutathione transferase 1. Anal Biochem. 2009; 390:52–56. [PubMed: 19348782]
21. Zhou WH, Shultz JW, Murphy N, Hawkins EM, Bernad L, Good T, Moothart L, Frackman S, Klaubert DH, Bulleit RF, Wood KV. Electrophilic aromatic substituted luciferins as bioluminescent probes for glutathione *S*-transferase assays. Chem Commun. 2006:4620–4622.
22. Yasgar A, Shultz J, Zhou WH, Wang H, Huang F, Murphy N, Abel EL, DiGiovanni J, Inglese J, Simeonov A. A high-throughput 1,536-well luminescence assay for glutathione *S*-transferase activity. Assay Drug Dev Technol. 2010; 8:200–211. [PubMed: 20085484]
23. Khambay, BPS.; Jewess, PJ. Comprehensive Molecular Insect Science. Khambay, BPS.; Jewess, PJ., editors. Vol. 6. Elsevier; Oxford: 2005. p. 1-30.
24. Vontas, J.; Ranson, H.; Williamson, MS. Insect Control, Biological and Synthetic Agents. Vontas, J.; Ranson, H.; Williamson, MS., editors. Elsevier; Oxford: 2010. p. 30-34.
25. Samra AI, Kamita SG, Yao Y-W, Cornel AJ, Hammock BD. Cloning and characterization of two glutathione *S*-transferases from pyrethroid-resistant *Culex pipiens*. Pest Manag Sci. 2012; 68:764–772. [PubMed: 22290868]
26. McAbee RD, Kang KD, Stanich MA, Christiansen JA, Wheelock CE, Inman AD, Hammock BD, Cornel AJ. Pyrethroid tolerance in *Culex pipiens pipiens* var *molestus* from Marin County, California. Pest Manag Sci. 2004; 60:359–368. [PubMed: 15119598]
27. Harper S, Speicher DW. Expression and purification of GST fusion proteins. Curr Protoc Protein Sci. 2008; 52:6.6.1–6.6.28. [PubMed: 18491301]
28. Mastropaolo W, Yourno J. An ultraviolet spectrophotometric assay for a-naphthyl acetate and a-naphthyl butyrate esterases. Anal Biochem. 1981; 115:188–193. [PubMed: 7304943]
29. Kamita SG, Samra AI, Liu JY, Cornel AJ, Hammock BD. Juvenile hormone (JH) esterase of the mosquito *Culex quinquefasciatus* is not a target of the JH analog insecticide methoprene. PLoS ONE. 2011; 6:e28392. [PubMed: 22174797]
30. Abdel-Aal YAI, Hammock BD. 3-Octylthio-1,1,1-trifluoro-2-propanone, a high affinity and slow binding inhibitor of juvenile hormone esterase from *Trichoplusia ni* (Hubner). Insect Biochem. 1985; 15:111–122.
31. Mahajan SS, Hou L, Doneanu C, Paranji R, Maeda D, Zebala J, Atkins WM. Optimization of bivalent glutathione *S*-transferase inhibitors by combinatorial linker design. J Am Chem Soc. 2006; 128:8615–8625. [PubMed: 16802828]
32. Parkinson, A. Casarett & Doull's Toxicology: The Basic Science of Poisons. Parkinson, A., editor. McGraw-Hill Companies, Inc; New York: 2001. p. 218-219.
33. Grant DF, Matsumura F. Glutathione *S*-transferase *Aedes aegypti* larvae - purification and properties. Insect Biochem. 1988; 18:615–622.
34. Pospischil R, Szomm K, Londershausen M, Schroder I, Turberg A, Fuchs R. Multiple resistance in the larger house fly *Musca domestica* in Germany. Pestic Sci. 1996; 48:333–341.
35. Wu DX, Scharf ME, Neal JJ, Suiter DR, Bennett GW. Mechanisms of fenvalerate resistance in the German cockroach, *Blattella germanica* (L.). Pestic Biochem Physiol. 1998; 61:53–62.
36. Kostaropoulos I, Papadopoulos AI, Metaxakis A, Boukouvala E, Papadopoulou-Mourkidou E. Glutathione *S*-transferase in the defence against pyrethroids in insects. Insect Biochem Mol Biol. 2001; 31:313–319. [PubMed: 11222940]
37. Vontas JG, Small GJ, Hemingway J. Glutathione *S*-transferases as antioxidant defence agents confer pyrethroid resistance in *Nilaparvata lugens*. Biochem J. 2001; 357:65–72. [PubMed: 11415437]
38. Vontas JG, Small GJ, Nikou DC, Ranson H, Hemingway J. Purification, molecular cloning and heterologous expression of a glutathione *S*-transferase involved in insecticide resistance from the rice brown planthopper, *Nilaparvata lugens*. Biochem J. 2002; 362:329–337. [PubMed: 11853540]

39. Yamamoto I, Kimmel EC, Casida JE. Oxidative metabolism of pyrethroids in houseflies. J Agric Food Chem. 1969; 17:1227.
40. Gaughan LC, Unai T, Casida JE. Permethrin metabolism in rats. J Agric Food Chem. 1977; 25:9–17. [PubMed: 1002942]
41. Ruzo LO, Unai T, Casida JE. Decamethrin metabolism in rats. J Agric Food Chem. 1978; 26:918–925. [PubMed: 670573]
42. Cole LM, Ruzo LO, Wood EJ, Casida JE. Pyrethroid metabolism: comparative fate in rats of tralomethrin, tralocythrin, deltamethrin, and (1*R*,a*S*)-*cis*-cypermethrin. J Agric Food Chem. 1982; 30:631–636. [PubMed: 6811643]
43. Soderlund DM, Hessney CW, Jiang M. Metabolism of fenvalerate by resistant Colorado potato beetles. J Agric Food Chem. 1987; 35:100–105.
44. Smith IH, Wood EJ, Casida JE. Glutathione conjugate of the pyrethroid tetramethrin. J Agric Food Chem. 1982; 30:598–600. [PubMed: 7096812]

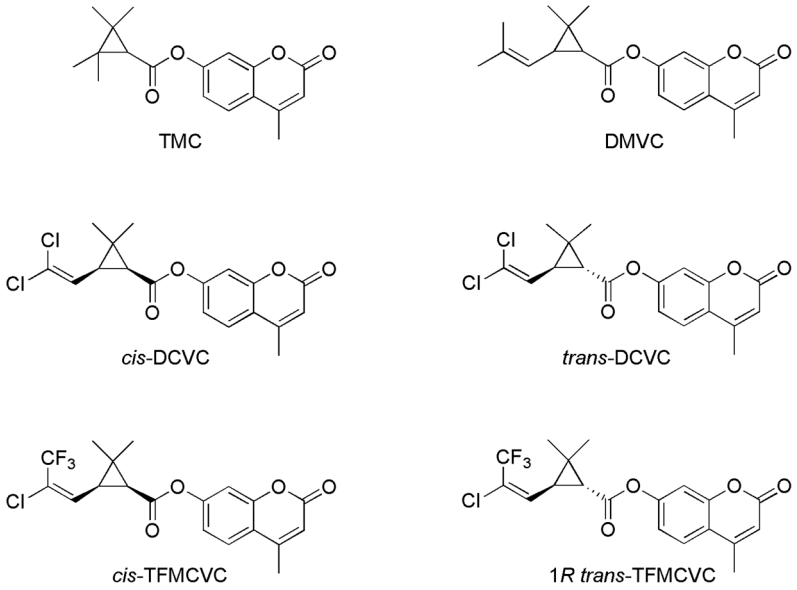

Fig. 1.

Chemical structures of the pyrethroid-like ester compounds generated and studied in this study. Abbreviations: **TMC**, 4-methyl-2-oxo-2H-chromen-6-yl, 2, 2, 3, 3-tetramethylcyclopropanecarboxylate; **DMVC**, 4-methyl-2-oxo-2H-chromen-6-yl, *cis*/*trans*-2,2-dimethyl-3-(2-methylprop-1-enyl) cyclopropanecarboxylate; ***cis*-DCVC**, 4-methyl-2-oxo-2H-chromen-6-yl, *cis*-3-(2,2-dichlorovinyl)-2,2-dimethylcyclo propanecarboxylate; ***trans*-DCVC**, 4-methyl-2-oxo-2H-chromen-6-yl, *trans*-3-(2,2-dichlorovinyl)-2,2-dimethyl cyclopropanecarboxylate; ***cis*-TFMCVC**, 4-methyl-2-oxo-2H-chromen-6-yl, *cis*-3-((Z)-2-chloro-3,3,3-trifluoroprop-1-enyl)-2,2-dimethylcyclopropanecarboxylate; **1*R trans*-TFMCVC**, 4-methyl-2-oxo-2H-chromen-6-yl, 1*R trans*-3-((Z)-2-chloro-3,3,3-trifluoroprop-1-enyl)-2,2-dimethylcyclopropanecarboxylate.

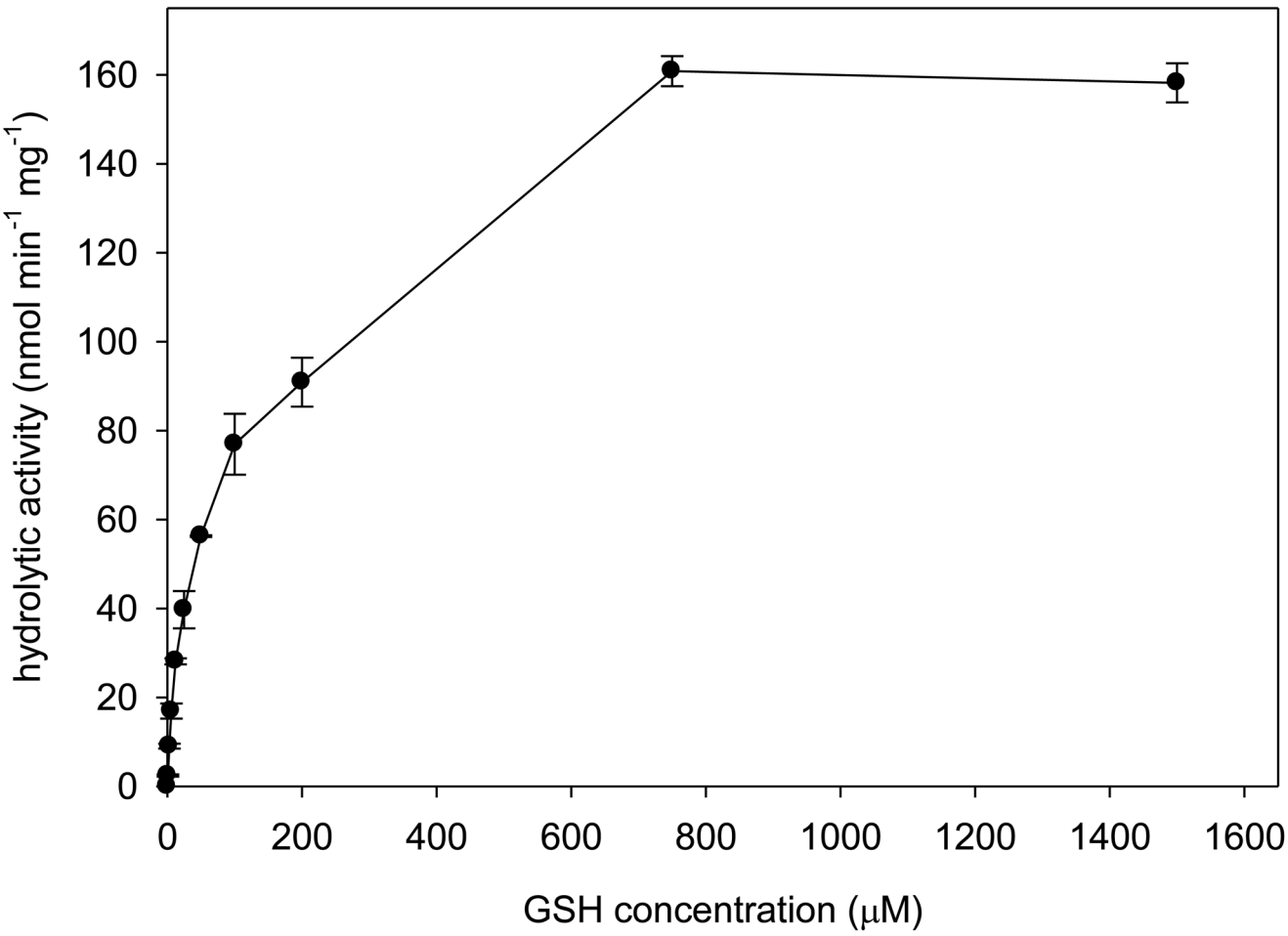

Fig. 2.

The effect of glutathione concentration on CpGSTD1 metabolic activity towards *cis*-DCVC. The reactions were performed in 90 mM sodium phosphate buffer, pH 7.4, containing 79 ng of CpGSTD1, 50 μM *cis*-DCVC, various concentrations of GSH (0.78 to 1,500 μM), and 2% (v/v) DEGEE at 34°C.

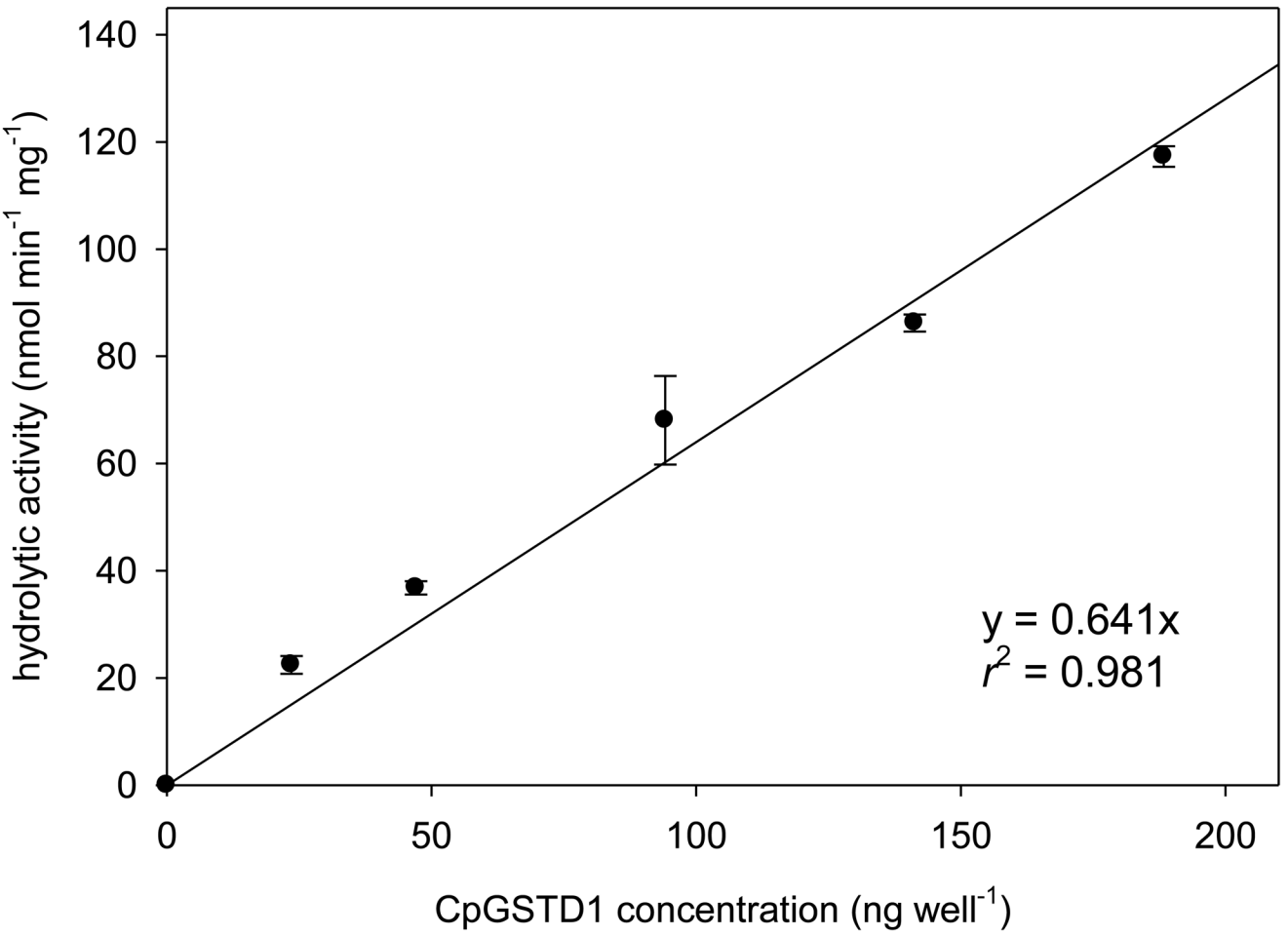

Fig. 3.

Correlation between GST activity and protein concentration. The reactions were performed in 90 mM sodium phosphate buffer, pH 7.4, containing various amounts of CpGSTD1 (23.5 to 188 ng), 50 μM *cis*-DCVC, 750 μM GSH, and 2% (v/v) DEGEE at 34°C.

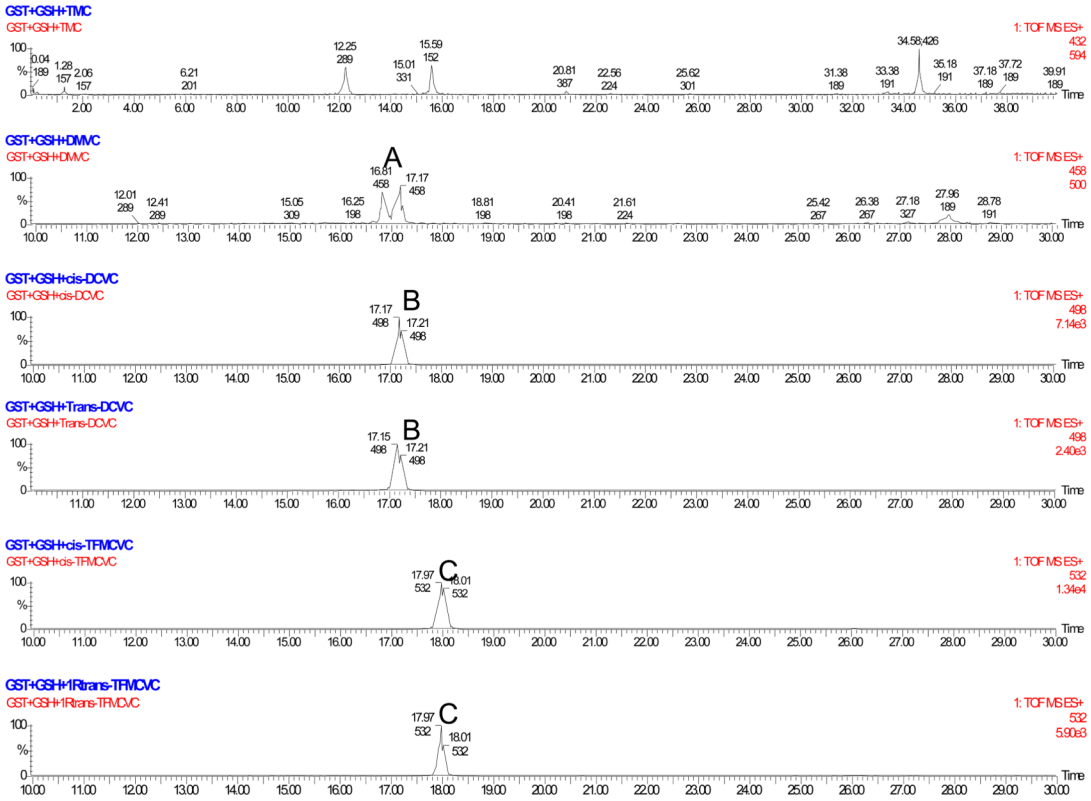

Fig. 4.

LC/MS ESI$^+$ profiles of the metabolites of the pyrethroid-like ester compounds following incubation with CpGSTD1. The reactions were performed in 90 mM sodium phosphate buffer, pH 7.4, containing 720 ng of CpGSTD1, fluorescent substrate (50 μM), 750 μM GSH, and 2% (v/v) DEGEE at 34°C. The profiles are from top to bottom: TMC, DMVC, *cis*-DCVC, *trans*-DCVC, *cis*-TFMCVC, and 1*R trans*-TFMCVC. Peaks corresponding to the predicted mass (*m*/*z*) of the GS-conjugates of DMVC, *cis*-/*trans*-DCVC, and *cis*-/*trans*-TFMCVC are indicated by the letters A (*m*/*z* 458 Da), B (*m*/*z* 498 Da), and C (*m*/*z* 532 Da), respectively. A peak corresponding to the predicted mass (*m*/*z* 432 Da) of the GSH-conjugated acid metabolite of TMC was not detected.

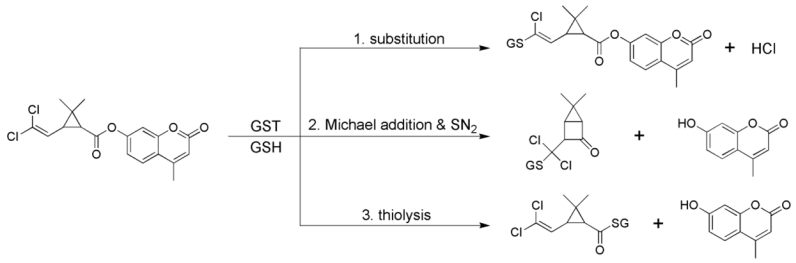

Fig. 5.

Three potential mechanisms of the metabolism of our pyrethroid-like ester compound DCVC by GST involving halogen substitution, Michael addition, and thiolysis.

Table 1

Specific activity of CpGSTD1 and mouse GSTs toward pyrethroid-like substrates

Substrate	Specific Activity[a] (nmol min^{-1} mg^{-1})	
	CpGSTD1	murine GSTs
TMC	10.5 ± 1.0	n.d.
DMVC	37.7 ± 7.6	n.d.
cis-DCVC	134 ± 12	3.5 ± 0.3
trans-DCVC	79.5 ±5.2	3.9 ± 0.4
cis-TFMCVC	233 ±9.9	1.4 ± 0.2
1*R trans*-TFMCVC	44.3 ± 5.6	4.0 ± 0.6
CDNB	98,000 ± 4,000	33,700 ± 2,000

[a]The enzyme assays were performed in 90 mM sodium phosphate, pH 7.4, buffer containing 720 ng of CpGSTD1 or 1,400 ng of mouse GSTs, 50 μM substrate, 750 μM GSH, and 0.5% (v/v) DEGEE at 34°C. The values are corrected for background hydrolysis. The results shown are the mean ± standard deviation of four replicates. The “n.d.” indicates that no activity was detected above background hydrolysis.

Table 2

Enzyme kinetic properties of CpGSTD1 with pyrethroid-like fluorescent and spectrophotometric substrates[a]

Substrate	V_{max} (nmol min^{-1} mg^{-1})	K_M (μM)	k_{cat} (s^{-1})	k_{cat}/K_M (M^{-1} s^{-1})
cis-DCVC	298 ± 13.6	9.0 ± 0.8	0.12	1.3×10^4
trans-DCVC	107 ± 4.5	5.9 ± 0.5	0.04	6.8×10^3
cis-TFMCVC	487 ± 14.0	10.0 ± 0.7	0.19	1.9×10^4
1*R trans*-TFMCVC	52.5 ± 1.5	5.0 ± 0.4	0.02	4.0×10^3
CDNB	102,000 ± 2,500	240 ± 18	40.4	1.7×10^5
DCNB	2,316 ± 152	691 ± 106	0.92	1.3×10^3

[a]The fluorescent enzyme assays were performed in 90 mM sodium phosphate, pH 7.4, buffer containing 184 ng of CpGSTD1, pyrethroid-like substrate (1 to 31.2 μM), 750 μM GSH, and 2% (v:v) DEGEE. The spectrophotometric assays were performed in 100 mM sodium phosphate, pH 6.5, buffer containing 100 ng of CpGSTD1, 5 mM substrate (CDNB or DCNB), 5 mM GSH, and 1.67% ethanol at 30°C. All of the values are corrected for background hydrolysis. The results shown are the mean ± standard deviation of four replicates.